RESEARCH ARTICLE

Open Access

A study on leakage current and electrical properties of oleic acid-coated cobalt-doped Mn-Zn ferrite nanocrystalline powders

M. Bhuvaneswari[1], S. Sendhilnathan[2], R. Tamilarasan[4*] and V. Sivakumar[3]

Abstract

Background: Mn-Zn ferrites have drawn a continuously an increasing interest because of their potential applications as multifunctional devices. These materials simultaneously exhibit ferroelectricity and ferromagnetism. The dielectric and leakage current properties of Cobalt substituted Mn-Zn ferrites coated with oleic acid were not reported.

Methods: This paper presents the synthesis, electrical, and leakage properties of nanoparticles of cobalt-doped Mn-Zn ferrite [$Co_xMn_yZn_yFe_2O_4$ (x = 0.1, 0.5, and 0.9 and y = 0.45, 0.25, and 0.05)] coated with oleic acid and prepared by chemical co-precipitation method. The crystal structure was determined by X-ray diffraction (XRD), the effect of strain on the electronic structure was analyzed using Williamson-Hall plot. Complex impedance spectroscopic analysis was carried out, and the impedance plots show the resistive and reactive parts of the impedance. Frequency dependence on AC conductivity was investigated for all the compositions, and leakage current properties were also studied.

Results: The nanoparticles were found to have an average size of 13.62 nm. The average crystallite size (D_{aveXR}) of the precipitated particles found to decrease from 15.22 to 12.65 nm with increasing cobalt substitution. The presence of two semicircular arcs at the lower and higher frequency regions indicates the grain boundary conduction and grain conduction at room temperature. Leakage current density of the order of 10^{-4} A/cm^2 (at field strength of 0.02 kV/cm) was observed for all compositions.

Conclusion: The variation of the strain values from negative to positive indicates that the strain changes from compression to tensile. The dielectric permittivity was found to decrease from 10^4 to 10^3 with increase in frequency. The semicircle in the higher frequency region is attributed to the grain conduction of the materials, and the semicircle in the lower frequency region is due to the grain boundary conduction. Both the grain and grain boundary are found to be active at room temperature. AC conductivity is found to be compositional dependent.

Keywords: Leakage current, Spinel, Nanoferrites, Co-precipitation

* Correspondence: rrtamilk@yahoo.co.in
[4]Department of Chemistry, Anna University Chennai -University College of Engineering, Pattukkottai, Rajamadam 614701, India
Full list of author information is available at the end of the article

Bhuvaneswari et al. Journal of Analytical Science and Technology (2017) 8:7

Page 2 of 8

Background

Mn-Zn ferrites are widely used in electronic applications, such as magnetic recording heads, transformers, choke coils, noise filters, electromagnetic gadgets, and memory or data storage devices (Dasgupta et al. 2006). Ferrimagnetic cubic spinels viz., ferrites possess properties of both magnetic materials and electric insulators making them an important material in many technological applications. Ferrites are preferred for their high permeability in the radio frequency region, high electrical resistivity, mechanical hardness, chemical stability, etc. (Zheng et al. 1998). Along with the development of science and technology, devices containing ferrites needed to get smaller in size for higher performance and the interest in soft magnetic materials therefore turned to the synthesis of nanocrystals and their substitutions, expecting to improve the properties (Yeong et al. 2003). Recently, cobalt ferrite nanoparticles were found to be photo-magnetic, exhibiting interesting light-induced coercivity changes (Arulmurugan et al. 2005) and Co-Zn ferrite was found to possess good elastic properties (Patil Sagar et al. 2009). Preparing stable colloidal suspensions of nanoparticles is challenging due to Vander Waal's forces and magnetic dipolar interactions. Hence, coating magnetic nanoparticles with a surfactant during chemical synthesis is essential in order to prepare well-dispersed nanoparticle colloids. Coating with oleic acid limits the growth of the nanoparticles and prevents the Ostwald ripening process as its surface layer acts as a barrier to mass transfer (Ayyappan et al. 2009; Davies et al. 1993). Oleic acid has also been widely used as a surfactant in the synthesis of mono dispersed nanoparticles (Tadmor et al. 2000), and it contains a carboxyl functional group that is used in bio applications, for example, to immobilize oligo nucleotides, and anti-cancer drug on particle surfaces (Kim et al. 2005; Somiya et al. 2003).

However, very less attention has been paid to the study of the electrical and leakage properties of cobalt-doped ferrite nanopowders coated with oleic acid. The investigations of electrical and leakage current properties of cobalt-doped ferrite nanopowders are thus important from the point of view of its use in electrical and electronic industry applications and hence the synthesis, leakage current properties, and the effects of strain on electrical properties are discussed in this report.

Methods

Apparatus and chemicals

The X-ray diffraction (XRD) patterns of the samples were recorded on a BRUKER-binary V2 (RAW) powder diffractometer using CuKα (λ = 1.5406 Å) radiation. The V-I characteristics were studied using KEITHLEY 6517A Electrometer/High Resistance Meter and the dielectric properties were studied using HIOKI 3532-50 LCR HITESTER.
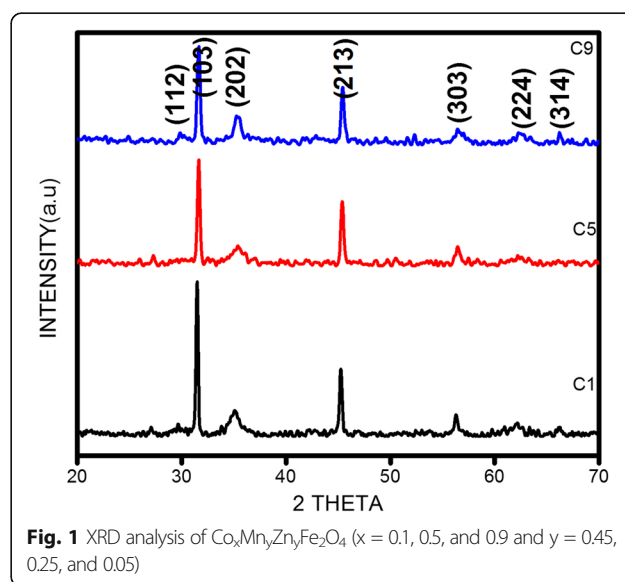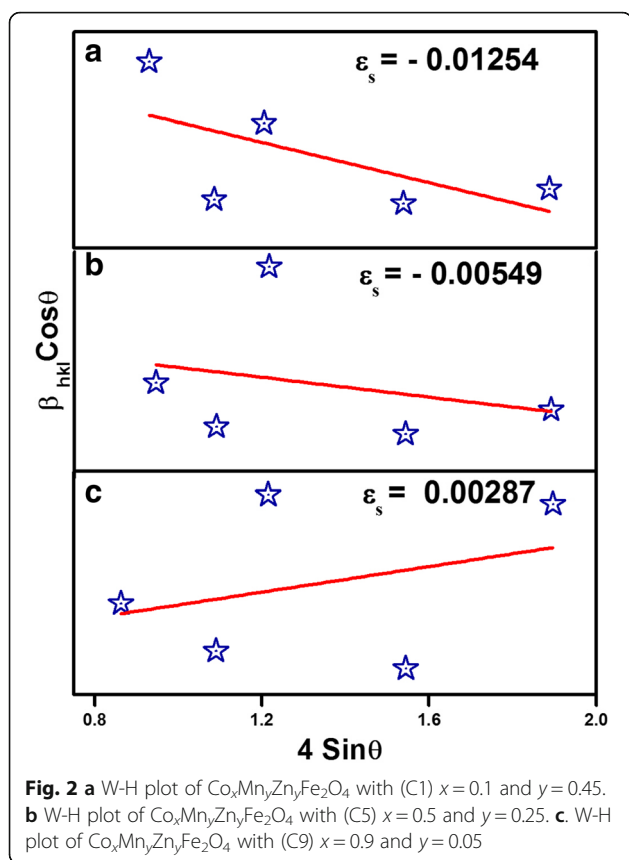
The materials that were procured for synthesizing the samples were of high grade purity. The synthesis of the nanoferrite material was done by the chemical co-precipitation method. For synthesizing the nano ferrite particles from the pure chemicals the salts of constituent metals were taken as starting materials. Sodium hydroxide (NaOH), a reducing agent was used as a base. The chemicals, Cobalt II chloride ($CoCl_2.6H_2O$), Manganese chloride ($MnCl_2.4H_2O$), Zinc chloride ($ZnCl_2$), Iron (III) Chloride ($FeCl_3.6H_2O$) were purchased from Merck, India. All the chemicals used were of analytical grade.

Synthesis of cobalt-doped Mn-Zn ferrites coated with oleic acid

The cobalt-doped ferrite nanoparticles synthesized by co-precipitation depends mostly on parameters viz., reaction temperature, pH of the suspension, initial molar concentration etc., (Jeyadevan et al. 2003). Ultra fine particles of $Co_xMn_y Zn_yFe_2O_4$ (x = 0.1, 0.5, and 0.9 and y = 0.45, 0.25, and 0.05) were prepared by co-precipitating aqueous solutions of $CoCl_2$, $MnCl_2$, $ZnCl_2$, and $FeCl_3$ mixtures in alkaline medium in their respective stoichiometric ratios at 333 K (60 °C).

This mixture was added to a boiling solution of NaOH (0.1 M dissolved in 1000 ml of distilled water) under constant stirring. Nanoferrites are formed due to the conversion of metal salts into hydroxides that take place immediately, followed by the transformation of hydroxides into ferrites. The solutions were maintained at 358 K (85 °C) for 1 h, and sufficient amount of fine particles were collected at this stage using magnetic separation. The particles were washed several times with distilled water followed by washing with acetone and are

Fig. 1 XRD analysis of $Co_xMn_yZn_yFe_2O_4$ (x = 0.1, 0.5, and 0.9 and y = 0.45, 0.25, and 0.05)

Bhuvaneswari *et al. Journal of Analytical Science and Technology* (2017) 8:7

Page 3 of 8

Fig. 2 a W-H plot of $Co_xMn_yZn_yFe_2O_4$ with (C1) $x = 0.1$ and $y = 0.45$. **b** W-H plot of $Co_xMn_yZn_yFe_2O_4$ with (C5) $x = 0.5$ and $y = 0.25$. **c**. W-H plot of $Co_xMn_yZn_yFe_2O_4$ with (C9) $x = 0.9$ and $y = 0.05$
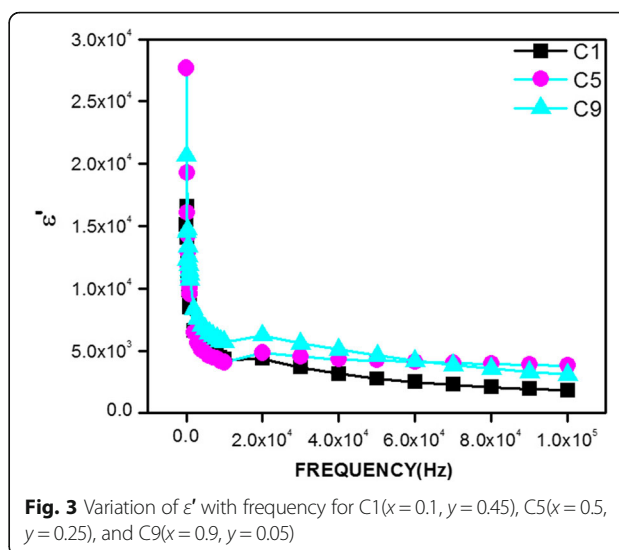
then dried at room temperature. For the preparation of the coated particles, a suitable surfactant (oleic acid) is added to the boiling solution of NaOH along with the solution mixture. The powdered samples were then pelletized at a pressure of 300 Kg/cm^2 to yield pellets of 10 mm diameter and approximately 2 mm thickness for all the three compositions.

Characterization

The X-ray diffraction (XRD) patterns of the samples were recorded on a BRUKER-binary V2 (RAW) powder diffractometer using CuKα ($\lambda = 1.5406$ Å) radiation. Slow scans of the selected diffraction peaks were carried out in step mode (step size 0.02°, measurement time 5s, measurement temperature 323 K (25 °C), standard; Si powder). The crystalline size of the nanocrystalline samples was measured using Debye-Scherrer

Table 1 Lattice constants, strain, and crystallite size of nanopowders

Sample	Lattice parameter (Å)			Volume of the unit cell (Å^3)	Strain (ε_s)	Crystallite size (nm)
	a	b	c			
C1	6.493	6.493	8.304	350.13	−0.01254	15.22
C5	5.652	5.652	10.732	342.83	−0.00549	13.01
C9	6.352	6.352	8.414	339.54	0.00287	12.65

Fig. 3 Variation of ε' with frequency for C1($x = 0.1$, $y = 0.45$), C5($x = 0.5$, $y = 0.25$), and C9($x = 0.9$, $y = 0.05$)
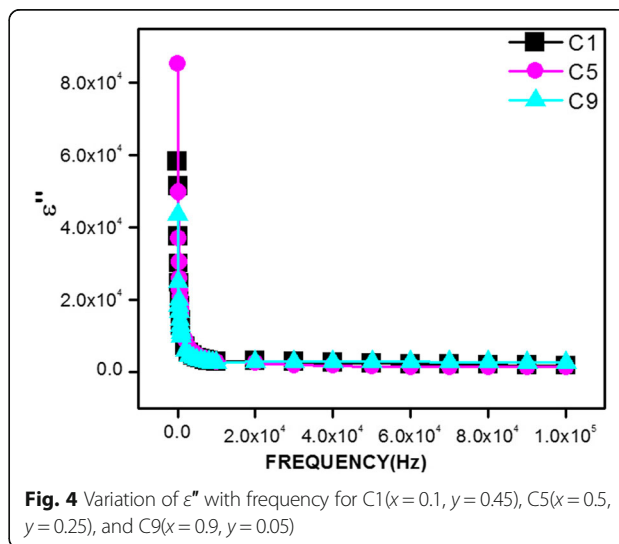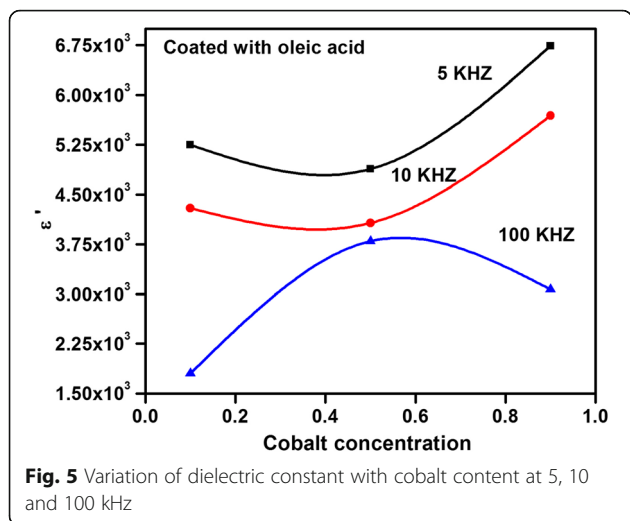
formula. The V-I characteristics were studied using KEITHLEY 6517A Electrometer/High Resistance Meter and the dielectric properties were studied using HIOKI 3532-50 LCR HITESTER.

Results and discussion

Structural characterization

The precipitated fine particles were characterized by XRD for structural determination and estimation of crystallite size. The XRD patterns were analyzed using JCPDS with all the peaks matching with the theoretically generated file (PDF#871171) and indexed. Analysis of the diffraction pattern using powder-X software (Creanga and Calugaru 2005) confirms the formation of tetragonal spinel structure in all the samples. The X-ray diffraction patterns (Fig. 1) of Co-doped Mn-Zn ferrites [$Co_xMn_yZn_y$-Fe_2O_4 ($x = 0.1$, 0.5, and 0.9 and $y = 0.45$, 0.25, and 0.05)

Fig. 4 Variation of ε'' with frequency for C1($x = 0.1$, $y = 0.45$), C5($x = 0.5$, $y = 0.25$), and C9($x = 0.9$, $y = 0.05$)

Bhuvaneswari *et al. Journal of Analytical Science and Technology* (2017) 8:7

Page 4 of 8

Fig. 5 Variation of dielectric constant with cobalt content at 5, 10 and 100 kHz

(C1, C5, C9)] coated with oleic acid indicate that the functionalization does not degrade the core cobalt ferrite (Andrade et al. 2014).

The broadening of XRD peaks shows refinement of grains and the strain associated with the nanocrystalline material. Williamson and Hall (W-H) proposed a method of deconvoluting size and strain from the mathematical expression,
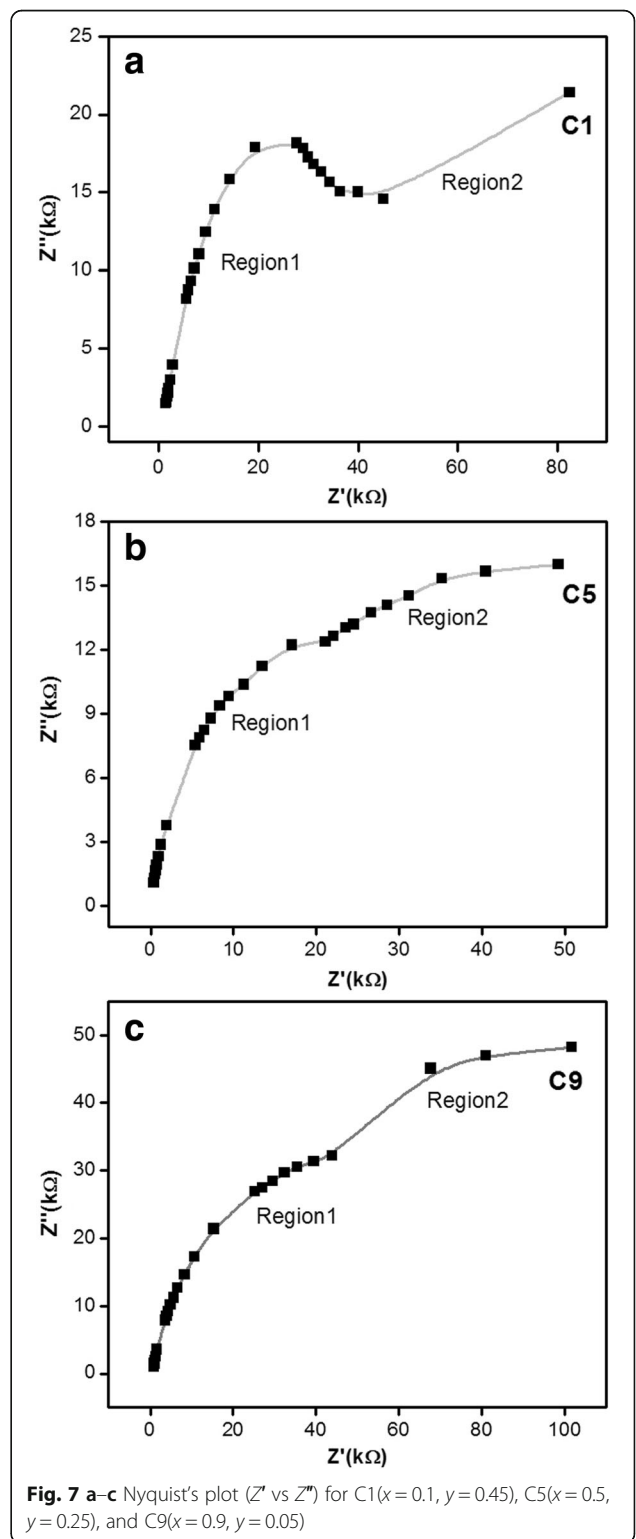
$$\beta_{hkl}\ cos\theta = \left[\frac{k\lambda}{D}\right] + 4\varepsilon_s\ sin\theta \qquad (1)$$

where k is the shape factor, λ is the X-ray wavelength, θ is the Bragg angle, D is the effective crystallite size (calculated by Debye-Scherrer equation), ε_s is the strain,
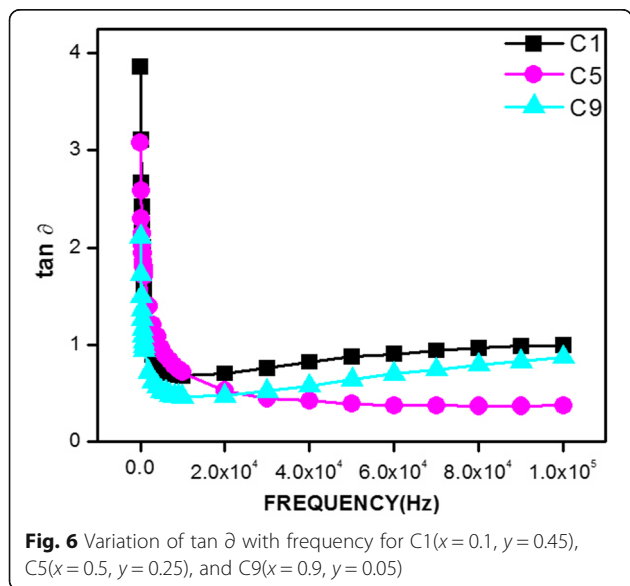
and β_{hkl} is the full width at half maximum of the corresponding hkl plane.

A plot drawn between *4 sinθ* along the X-axis and β_{hkl} *cosθ* along the Y-axis is shown in Fig. 2a–c. From the data of linear fit, the value of strain was calculated from
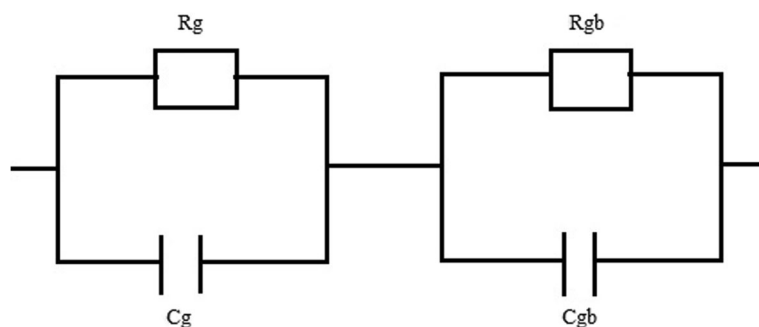

Fig. 7 a–c Nyquist's plot (Z' vs Z'') for C1(*x* = 0.1, *y* = 0.45), C5(*x* = 0.5, *y* = 0.25), and C9(*x* = 0.9, *y* = 0.05)

Fig. 6 Variation of tan ∂ with frequency for C1(*x* = 0.1, *y* = 0.45), C5(*x* = 0.5, *y* = 0.25), and C9(*x* = 0.9, *y* = 0.05)

Bhuvaneswari et al. Journal of Analytical Science and Technology (2017) 8:7

Page 5 of 8

Fig. 8 Equivalent circuit for Nyquist's plot (Z' vs Z'') for C1($x = 0.1$, $y = 0.45$), C5($x = 0.5$, $y = 0.25$), and C9($x = 0.9$, $y = 0.05$)

the slope of the line. Negative slope in plots a and b (Fig. 2a, b) indicates that the system is under compressive strain (Maurya et al. 2011). Positive slope in plot c (Fig. 2c) indicates that the system is under tensile strain. The average crystallite sizes of the prepared ferrite particles were calculated by means of the Debye-Scherrer equation (Sharma et al. 2005). The crystallite size was found to decrease with increase in cobalt content as was reported by many researchers (Zhang et al. 2009).

The lattice parameter, average crystallite size, and lattice strain are given in Table 1. From the table, strain (ε_s) values were found to be −0.01254 for $x = 0.1$, −0.00549 for $x = 0.5$ and 0.00287 for $x = 0.9$.

Dielectric studies

Figures 3 and 4 illustrate the frequency dependence of the real and imaginary part of the dielectric constants for all composition at room temperature. The dielectric constant decreases with increasing frequency exhibiting normal ferrimagnetic behavior for all the compositions (Smit and Wijn 1959). As the frequency increases, the dielectric constant remains almost constant. This is a normal behavior of ferrites and can be explained with the help of Maxwell-Wagener model (1951) (Wagner 1913).

Since the grain boundaries of lower conductivity are found to be effective at lower frequencies while the ferrite grains of high conductivity are effective at high frequencies (Koops 1951; Kumar and Srivastava 1994), higher values of ε' at lower frequencies and vice versa are observed. For example, the ε' values in the order of 10^4 in the frequency range 10^2 to 10^3 Hz decreases to the order of 10^3 with increasing frequency. The low dielectric values make these ferrites useful in high-frequency applications (Pathan and Shaikh 2012). The variation of dielectric constant with various concentrations of cobalt at 5, 10 and 100 KHz, for particles coated with oleic acid is shown in Fig. 5. At a frequency of 10 KHz, the dielectric constant was found to decrease slightly and then increase with increasing cobalt content

(Bhuvaneswari et al. 2016). However the dielectric constant increases and then decreases with increase in cobalt content at the frequency of 100 KHz which may be attributed to the corresponding changes in microstructures due to the coating of oleic acid.

Loss tangent

The loss tangent represents the energy dissipation of dielectric material. The variation of $tan\ \delta$ with frequency for various compositions at room temperature is shown in Fig. 6. The curves suggest that $tan\ \delta$ strongly depend on the applied frequency (Rani et al. 2013). The dielectric loss decreases rapidly with frequency up to 10 kHz for all the compositions. For the composition $Co_{0.5}Mn_{0.25}Zn_{0.25}Fe_2O_4$ (C5), the loss was found to be very low (<0.4) at a frequency of 100 kHz.

The dependence of the imaginary part (ε'') with frequency is similar to that of the dielectric loss on frequency. This shows that ε'' is directly proportional to $tan\ \delta$ according to the following equation:
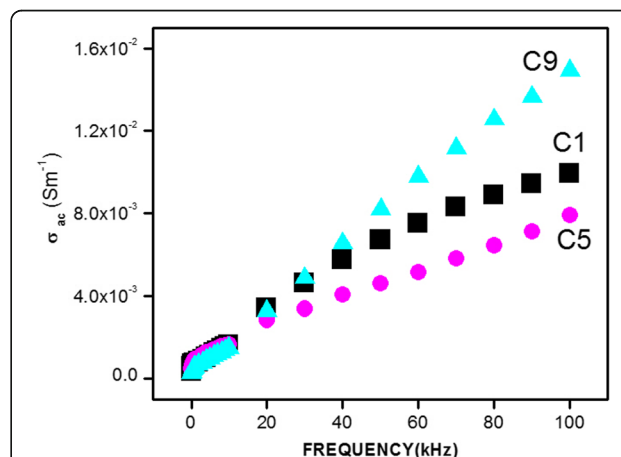
$$\varepsilon'' = \varepsilon' \tan\delta \qquad (2)$$

Fig. 9 Frequency vs AC conductivity for C1($x = 0.1$, $y = 0.45$), C5($x = 0.5$, $y = 0.25$), C9($x = 0.9$, $y = 0.05$) at room temperature

Bhuvaneswari *et al. Journal of Analytical Science and Technology* (2017) 8:7

Page 6 of 8

where ε'' is the imaginary part of dielectric, ε' is the real part and tan δ is the dielectric loss. ε' was calculated using the following equation.

$$\varepsilon' = \frac{C\,d}{\varepsilon_0 A} \tag{3}$$

Fig. 10 Leakage current density of coated particle as a function of electric field of **a** $Co_{0.1}$ $Mn_{0.45}Zn_{0.45}Fe_2O_4$, **b** $Co_{0.5}$ $Mn_{0.25}Zn_{0.25}Fe_2O_4$, and **c** $Co_{0.9}$ $Mn_{0.05}Zn_{0.05}Fe_2O_4$

where $\varepsilon_0 = 8.854 \times 10^{-12}$ *F/m* is the absolute permittivity of free space, C is the capacitance, A is the area, and d is the thickness.

Impedance analysis

Impedance spectroscopy is a relevant technique to obtain information about the electrical behavior of nano- and polycrystalline materials as the impedance measurement data gives both resistive (real) and reactive (imaginary) components. To separate the grain and grain boundary contributions of the cobalt-doped Mn-Zn ferrite samples, complex impedance plane plots (Cole-Cole plots) have been drawn in the frequency range from 100Hz to 100 KHz at room temperature. One or two successive semicircles may occur due to grain or grain boundaries. These contributions can conventionally be displayed in a complex plane plots (Nyquist diagram) in terms of the formalism.

Complex impedance is given by as follows:

$$Z^*(\omega) = Z' - jZ'' \tag{4}$$

where $Z' = |Z|\cos\theta$ and $Z'' = |Z|\sin\theta$. In Fig. 7a–c, two semicircles are seen for all compositions [$Co_xMn_yZn_y$ Fe_2O_4 ($x = 0.1$, 0.5, and 0.9 and $y = 0.45$, 0.25, and 0.05)] even at room temperature. The semicircle in the higher frequency region is attributed to the grain conduction of the materials which occurs due to parallel combination of the grain resistance R_g and grain capacitance C_g of the material. The semicircle in the lower frequency region is attributed to the grain boundary conduction which occurs due to parallel combination of the grain boundary resistance R_{gb} and grain boundary capacitance C_{gb} of the material (Barik et al. 2011; Dasari et al. 2011). These two semicircles can be modeled by two parallel RC equivalent circuits in series configuration as shown in Fig. 8. It is noticed that the circular arcs in the lower and higher frequency regions are not completed which may be due to the fact that grain boundary resistance and grain resistance are out of measurement scale (Ali et al. 2015).

AC conductivity

Figure 9 shows the frequency dependence of AC conductivity at room temperature. The curves suggest that the values of AC conductivity increases gradually with increase in frequency, which is the normal behavior of ferrites (Sathishkumar et al. 2010). The increase in AC conductivity with applied field can be explained on the basis of pumping force of the applied field which promotes the transfer of charge carriers between the two Fe ion states and also the liberation of charges from different trapping centers. These charge carriers along with electrons produced from the valence exchange between different metal ions participate in conduction process. From
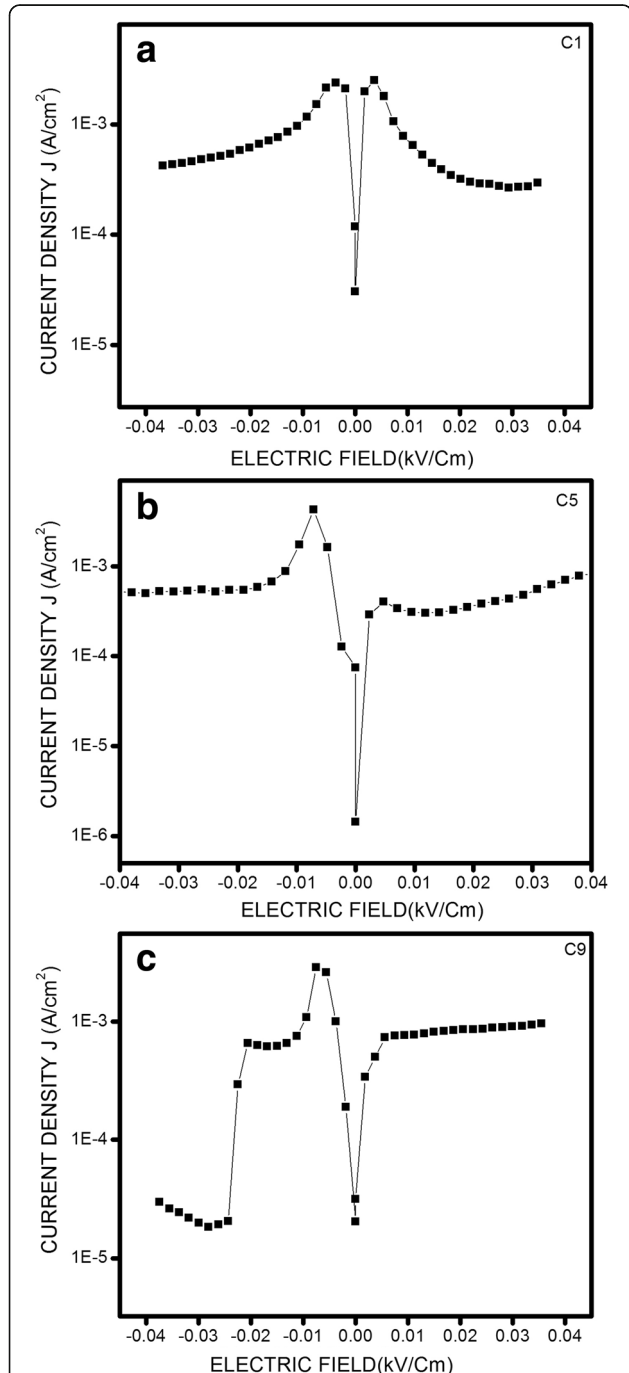
Fig. 9, it is evident that AC conductivity is higher for the composition $Co_{0.9}Mn_{0.05}Zn_{0.05}Fe_2O_4$ indicating that AC conductivity is compositional dependent (Batoo 2011).

Leakage current density

The leakage current density (J) is measured as a function of applied field for all the compositions as shown in Fig. 10a–c. For a given applied voltage, the current was found to decay with time and the measurements were taken after the stabilization of current. The V-I characteristic curves show the voltage polarity dependence (Stolichnov et al. 2000). For coated particles, a low leakage current density of the order of 10^{-4} A/cm^2 is measured at a field strength of 0.02 kV/cm.

Conclusions

From the above study it could be seen that the oleic acid prevents agglomeration of the cobalt ferrite nanoparticles, and their crystallinity is not affected by the oleic acid coating. The crystallite size was found to decrease with increase in cobalt content, and the micro strain values of materials identified from the Williamson-Hall plot model shows all the samples having a very low value of micro strain due to calcinations. The variation of the strain values from negative to positive indicates that the strain changes from compression to tensile. The dielectric permittivity was found to decrease from 10^4 to 10^3 with increase in frequency. The variation in the behavior of dielectric constant with cobalt concentration at 10 and 100 KHz may be attributed to the changes in microstructures due to the coating of oleic acid. The dielectric loss was found to decrease with frequency up to 10 KHz for all the compositions, and the loss was found to be very low (<0.4) at a frequency of 100 KHz for the composition $Co_{0.5}$ $Mn_{0.25}Zn_{0.25}Fe_2O_4$ (C5). The impedance spectroscopy analysis shows two semicircular regions for all the compositions even at room temperature. The semicircle in the higher frequency region is attributed to the grain conduction of the materials, and the semicircle in the lower frequency region is due to the grain boundary conduction. Both the grain and grain boundary are found to be active at room temperature. The AC conductivity is observed to increase gradually with the increase in frequency, which is the normal behavior expected of ferrites. AC conductivity was found to be higher for the composition $Co_{0.9}Mn_{0.05}Zn_{0.05}Fe_2O_4$ indicating compositional dependence of AC conductivity. A low leakage current density of the order of 10^{-4} A/cm^2 was also observed at a field strength of 0.02 kV/cm for all compositions.

Authors' contributions
MB carried out the all the experimental work, RT participated in the interpretation of experimental and analysis, and VS participated in the sequence alignment and drafted the manuscript. SS participated in its design and coordination and helped to draft the manuscript. All authors read and approved the final manuscript.

Competing interests
The all authors declare that they have no competing interests.

Publisher's Note
Springer Nature remains neutral with regard to jurisdictional claims in published maps and institutional affiliations.

Author details
[1]Department of Physics, MNSK College of Engineering, Pudukkottai 622305, India. [2]Department of Physics, Anna University Chennai: University College of Engineering, Pattukkottai, Rajamadam 614701, India. [3]Department of Physics, Anna University -BIT Campus, Tiruchirappalli 620024, India. [4]Department of Chemistry, Anna University Chennai -University College of Engineering, Pattukkottai, Rajamadam 614701, India.

References
Ali MA, Khan MNI, Chowdhury FUZ, Akhter S, Uddin MM. Structural properties, impedance spectroscopy and dielectric spin relaxation of Ni-Zn ferrite synthesized by double sintering technique. J Sci Res. 2015;7:65–75.

Andrade PL, Silva VAJ, Maciel JC, Santillan MM, Moreno NO, Santos DL Valladares L, Bustamante A, Pereira SMB, Silva MPC, Albino A. Hyperfine Interactions. ISSN: 0304-3843 (Print) 1572-9540 (Online): Springer; 2014. doi:10.1007/s10751-013-0835-4.

Arulmurugan R, Vaidyanathan G, Senthilnathan S, Jeyadevan B. Co–Zn ferrite nanoparticles for ferrofluid preparation: study on magnetic properties. Phys B Condens Matter. 2005;363:225–31.

Ayyappan S, Philip J, Raj B. Formation of ferrimagnetic films with functionalized magnetite nanoparticles using the Langmuir–Blodgett technique. J Phys Chem C. 2009;113:590–6.

Barik SK, Choudhary RNP, Singh AK. AC impedance spectroscopy and conductivity studies of BaO. 8SrO. 2TiO$_3$ ceramics. Adv Mater Lett. 2011;2:419–24.

Batoo KM. Study of dielectric and impedance properties of Mn ferrites. Physica B. 2011;406:382–7.

Bhuvaneswari M, Sendhilnathan S, Kumar M, Tamilarasan R, Giridharan NV. Synthesis, investigation on structural and electrical properties of cobalt doped Mn–Zn ferrite nanocrystalline powders. Mater Sci Pol. 2016;34:344–53.

Creanga D, Calugaru G. Physical investigations of a ferrofluid based on hydrocarbons. J Magn Mater. 2005;289:81–3.

Dasari MP, Rao KS, Krishna PM, Krishna GG. Barium strontium bismuth niobate layered perovskites: dielectric. Impedance and Electrical Modulus Characteristics Acta Physica Polonica A. 2011;119:387–94.

Dasgupta S, Kim KB, Ellrich J, Eckert J, Manna I. Mechano-chemical synthesis and characterization of microstructure and magnetic properties of nanocrystalline Mn$_{1-x}$Zn$_x$Fe$_2$O$_4$. J Alloys Compd. 2006;424:13–20.

Davies KJ, Wells S, Charles SW. The effect of temperature and oleate adsorption on the growth of maghemite particles. J Magn Mater. 1993;122:24–8.

Jeyadevan B, Chinnasamy CN, Shinoda K, Tohji K, Oka H. Mn-Zn ferrite with higher magnetization for temperature sensitive magnetic fluid. J App Phy. 2003;93:8450–2.

Kim DH, Lee SH, Kim KN, Kim KM, Shin IB, Lee YK. Cytotoxicity of ferrite particles by MTT and agar diffusion methods for hyperthermic application. Magn Magn Mater. 2005;293:287–92.

Koops CG. On the dispersion of resistivity and dielectric constant of some semiconductors at audio frequencies. Phys Rev. 1951;83:121.

Kumar B, Srivastava G. Dispersion observed in electrical properties of titanium substituted lithium ferrites. J Appl Phys. 1994;75:6115(1994).

Maurya A, Chauhan P, Mishra SK, Srivastava RK. Structural, optical and charge transport study of rutile TiO$_2$ nanocrystals at two calcination temperatures. J Alloys Compd. 2011;509:8433–40.

Bhuvaneswari *et al. Journal of Analytical Science and Technology* (2017) 8:7

Page 8 of 8

Pathan AT, Shaikh AM. Dielectric properties of Co-substituted Li-Ni-Zn nanostructured ferrites prepared through chemical route. Int J Computer Appl. 2012;45:0975–8887.

Patil VG, Shirsath Sagar E, More SD, Shukla SJ, Jadhav KM, Effect of zinc substitution on structural and elastic properties of cobalt ferrite. J Alloys Compd. 2009;488:199–203.

Rani R, Kumar G, Batoo KM, Singh M. Electric and dielectric study of zinc substituted cobalt nanoferrites prepared by solution combustion method. American J Nanomaterials. 2013;1:9–12.

Sathishkumar G, Venkataraju C, Sivakumar K. Synthesis, structural and dielectric studies of nickel substituted cobalt-zinc ferrite. Mat Sci Appl. 2010;1:19–24.

Sharma RK, Suwalka O, Lakshmi N. Synthesis of chromium substituted nano particles of cobalt zinc ferrites by coprecipitation. Mater Lett. 2005;59:3402–5.

Smit J, Wijn HPJ. Ferrites: physical properties of ferromagnetic oxides in relation to their technical applications. Eindhoven: Philips technical Library; 1959. p. 158.

Somiya S, Aldinger S, Claussen N, Uchino RM, Koumto K, Kanenoin K. Handbook of advanced ceramics, Vol. II, processing and their applications. Waltham: Elsevier Academic Press; 2003. p. 394.

Stolichnov I, Tagantsev A, Setter N, Okhonin S, Fazan P, Cross JS, Sukada MT. Dielectric breakdown in (Pb, La)(Zr, Ti) O_3 ferroelectric thin films with Pt and oxide electrodes. J Appl Phys. 2000;87:1925–31.

Tadmor R, Rosensweig RE, Frey J, Klein J. Resolving the puzzle of ferrofluid dispersants. Langmuir. 2000;16:9117–20.

Wagner KW. Zur Theorie der unvollkommenen Dielektrika. Ann Phys, (Leipzig). 1913;40:817.

Yeong Il K, Don K, Lee C s. Synthesis and characterization of $CoFe_2O_4$ magnetic nanoparticles prepared by temperature-controlled coprecipitation method. Phys B Condens Matter. 2003;337:42–51.

Zhang CF, Zhong XC, Yu HY, Liu ZW, Zeng DC. Effects of cobalt doping on the microstructure and magnetic properties of Mn–Zn ferrites prepared by the co-precipitation method. Physica B. 2009;404:2327–31.

Zheng M, Wu XC, Zou BS, Wang YJ. Magnetic properties of nanosized $MnFe_2O_4$ particles. J Magn Magn Mater. 1998;183:152–6.